PROCEEDINGS of the
23rd International Congress on Acoustics

9 to 13 September 2019 in Aachen, Germany

Moving sources and the 2.5D Helmholtz boundary element method

Christian H. KASESS(1), Holger WAUBKE(2)

(1)Acoustics Research Institute, Austrian Academy of Sciences, Austria, christian.kasess@oeaw.ac.at

(2)Acoustics Research Institute, Austrian Academy of Sciences, Austria, holger.waubke@oeaw.ac.at

Abstract

For perception tests on environmental noise, e.g. evaluating the effect of a noise barrier, it can become necessary to virtualize moving sources. In the framework of the 2.5D boundary element method, used for long and large structures, the full treatment of sources moving along the length of the structure is possible but can become computationally quite involved. Even in the simplest case, i.e. mono-frequent emission and constant speed, higher speeds require calculations for ever higher 2D frequencies beyond the 3D target frequency in order to perform the necessary spatial inverse Fourier transform to acquire the time signal. For wide-band signals a 2D inverse Fourier transform needs to be performed for each point in time. Adding a further non-uniform motion results in yet another dimension that needs to be integrated over. For higher sampling frequencies and signal durations of a few seconds this can become problematic. Interpolation between data points in either frequency or space can help to decrease the computational burden in particular when employing different types of demodulation schemes. Initial data for a sampled source signal is presented to illustrate at which points in the calculation interpolation can be applied without introducing too high a computational error.

Keywords: moving source, Helmholtz equation, boundary element method

1 INTRODUCTION

In environmental noise research the boundary element method (BEM) is an important tool in particular for situations were simpler approaches such as those used in noise mapping are not sufficient e.g. for the evaluation of complex barrier designs [1] or other complicated cross-sections such as railway platforms with a canopy [2]. In order to reduce the computational burden, many of these applications involve the use of BEM approaches applying simplifying assumptions such as a constant cross-section as in the 2D BEM and nowadays in particular the more general 2.5D approaches [3, 4] which allow for more realistic source models. However, often the source models used are stationary point sources or incoherent line sources which do not take the motion of the source as in traffic into account. However, for perception tests on environmental noise, e.g. evaluating the effect of a noise barrier, it can become necessary to virtualize such moving sources.

In situations with a constant cross-section where 2.5D approaches are applicable, a mono-frequent source moving at a constant speed along the length of the structure can be treated quite efficiently [3]. Even in the 2.5D case as soon as non-uniform motion (acceleration or decelaration) and wide-band signals are concerned, the full treatment of moving sources becomes computationally involved. In this general setting, a three-dimensional integration needs to be performed comprising a forward Fourier transform and two inverse Fourier transforms. Whereas the temporal transforms can be treated as discrete Fourier transforms (DFT) in a relatively straightforward manner, this requires, first, a large number of 2D calculations and, second, the evaluation of many inverse Fourier transforms to the spatial domain. The aim of this work is to investigate whether, and to what degree, the number of calculations can be reduced by interpolating between data points. For this, also a demodulation in frequency and/or space is investigated similar to the method for the 2D calculations as suggested in [3] and successfully used in [4].

2 METHODS

2.1 2.5D Boundary element method

A brief overview on the treatment of a moving source in a 2.5D setting is provided. For more details the reader is referred to [3]. The starting point is the wave equation for the pressure p in the time domain of a source moving along the x-axis (i.e. the infinite dimension of the scatterer):

$$\nabla^2 p(\mathbf{x},t) - \frac{1}{c^2}\frac{\partial^2 p(\mathbf{x},t)}{\partial t^2} = -s(t)\delta(\mathbf{x}-\mathbf{x_0}(t)), \tag{1}$$

with c being the speed of sound. $\mathbf{x} = (x,y,z)^T$ and $\mathbf{x_0}(t) = (x_0(t), y_0, z_0)^T$ denote the point in space where the wave equation is evaluated and the source point, respectively. $s(t)$ is the source signal which will also be referred to as the signal. The Fourier transform along t and x leads to:

$$\begin{aligned}
&\nabla^2 p_2(y,z,\omega,k_x) - k_x^2 p_2(x,y,\omega,k_x) + k^2 p_2(x,y,\omega,k_x) = \\
&= -\left(\int_{-\infty}^{\infty}\int_{-\infty}^{\infty} s(t)\delta(x-x_0(t))e^{i\omega t}e^{-ik_x x}dxdt\right)\delta(y-y_0)\delta(z-z_0) \\
&= -\left(\int_{-\infty}^{\infty} s(t)e^{i\omega t}e^{-ik_x x_0(t)}dt\right)\delta(y-y_0)\delta(z-z_0) \\
&= -S(\omega,k_x)\delta(y-y_0)\delta(z-z_0),
\end{aligned} \tag{2}$$

with the 3D-wavenumber $k = \omega/c$ and the spatial wave number k_x. p_2 is used to indicate the pressure in 2D (y and z).

When the source is stationary then $S(\omega,k_x) = \hat{s}(\omega)e^{-ik_x x_0}$ resulting in a straightforward 2.5D problem with a source spectrum weighting and a phase factor depending on the x-offset. The inverse Fourier transform over k_x can be calculated as described e.g. in [4] or [3] leading to $\hat{p}(\mathbf{x},\omega)$.

For a moving source, the time signal at the receiver is often more interesting, which requires a second inverse Fourier transform over ω. Thus the solution of a source moving along direction x reads as follows:

$$\begin{aligned}
p(\mathbf{x},t) &= \frac{1}{(2\pi)^2}\int_{-\infty}^{\infty}\int_{-\infty}^{\infty} S(\omega,k_x)q(y,z,\omega,k_x)e^{-i\omega t}e^{ik_x x}dk_x d\omega \\
&= \frac{1}{(2\pi)^2}\int_{-\infty}^{\infty}\int_{-\infty}^{\infty}\left(\int_{-\infty}^{\infty} s(t')e^{i\omega t'}e^{-ik_x x_0(t')}dt'\right)q(y,z,\omega,k_x)e^{-i\omega t}e^{ik_x x}dk_x d\omega,
\end{aligned} \tag{3}$$

where $q(y,z,\omega,k_x) = q(y,z,\sqrt{(\omega/c)^2 - k_x^2})$ is the solution of the 2D-problem in the y-z plane.

2.2 Uniform motion

The simplest case is a uniform motion $x_0(t) = x_0 + vt$ of a mono-frequent source $s(t) = Ae^{-i\omega_0 t}$. To begin with, uniform motion leads to

$$\begin{aligned} p(\mathbf{x},t) &= \frac{1}{(2\pi)^2} \int_{-\infty}^{\infty}\int_{-\infty}^{\infty} \left(\int_{-\infty}^{\infty} s(t') e^{it(\omega + k_x v)} dt' \right) q(y,z,\omega,k_x) e^{-i\omega t} e^{ik_x x} dk_x d\omega \\ &= \frac{1}{(2\pi)^2} \int_{-\infty}^{\infty}\int_{-\infty}^{\infty} \hat{s}(\omega - k_x v) q(y,z,\omega,k_x) e^{-i\omega t} e^{ik_x x} dk_x d\omega, \end{aligned} \tag{4}$$

where x_0 is set to zero for simplicity. Thus, in the wavenumber domain, the source spectrum is shifted by $k_x v$. If the signal is a mono-frequent complex exponential, this simplifies further to [3]:

$$\begin{aligned} p(\mathbf{x},t) &= \frac{1}{(2\pi)^2} \int_{-\infty}^{\infty}\int_{-\infty}^{\infty} A\delta(\omega - \omega_0 - k_x v) e^{-ik_x x_0} q(y,z,\omega,k_x) e^{-i\omega t} e^{ik_x x} dk_x d\omega \\ &= \frac{1}{(2\pi)^2} e^{-i\omega_0 t} \int_{-\infty}^{\infty} A e^{-ik_x(x_0 + v - x)} q\left(y,z,\sqrt{((\omega_0 + k_x v)/c)^2 - k_x^2}\right) dk_x. \end{aligned} \tag{5}$$

The 2D-wavenumbers for which $q(.)$ needs to be evaluated are now given by $\sqrt{((\omega_0 + k_x v)/c)^2 - k_x^2}$. Thus, the integration is not symmetric with respect to k_x anymore as in the case of a stationary source. For $(\omega_0 + k_x v)/c)^2 - k_x^2 < 0$, i.e. $k_{x-} < -k(1+v/c)^{-1}$ and $k_{x+} > k(1-v/c)^{-1}$, the argument of the Hankel functions in the 2D BEM becomes imaginary and thus the Hankel function decays exponentially. Contrary to the stationary case, the evaluation of the above expression requires to evaluate 2D-BEM calculations beyond ω_0 up to $\omega_0 c(c^2 - v^2)^{-1/2}$. E.g. for 4000 Hz, a speed of 180 km/h, and the speed of sound being 343.5 m/s this results of an upper frequency bound of 4043.06 Hz. While this does not seem a large difference it is important to keep in mind that in particular the high frequencies require high computational effort and that the original quadrature grid may not be valid anymore, depending on the quadrature method. Importantly, as soon as the surfaces of the scatterer or the ground are not fully reflecting, each signal frequency ω_0 requires to calculate a full set of 2D solutions [5].

2.3 Sampling the source signal

When a sampled signal is used, the Fourier transform of the signal $s(t)$ is replaced by the discrete time Fourier transform (DTFT) of $s(t)e^{ik_x x_0(t)}$. Inserting this into Eq. 3 leads to :

$$\begin{aligned} p(\mathbf{x},t) &= \frac{1}{(2\pi)^2} \int_{-\infty}^{\infty}\int_{-\infty}^{\infty} \sum_{n=-\infty}^{\infty} s(nT_s) e^{i\omega nT} e^{-ik_x x_0(nT_s)} q(y,z,\omega,k_x) e^{-i\omega t} e^{ik_x x} dk_x d\omega \\ &= \frac{1}{(2\pi)^2} \sum_{n=-\infty}^{\infty} s(nT_s) \int_{-\infty}^{\infty} e^{-i\omega(t - nT_s)} \left(\int_{-\infty}^{\infty} q(y,z,\omega,k_x) e^{ik_x(x - x_0(nT_s))} dk_x \right) d\omega, \end{aligned} \tag{6}$$

where the expression in the parenthesis is the static 2.5D solution at ω and source-receiver offset $x - x_0(nT_s)$ which can be calculated as given e.g. in [4]. Thus, essentially the same set of 2D-calculations can be used to calculate the different 2.5D solutions. Clearly, for this to be feasible, the signal needs to be truncated in a suitable manner:

$$p(\mathbf{x},t) = \frac{1}{(2\pi)^2}\sum_{n=0}^{N-1} s(nT_s)\int_{-\infty}^{\infty} e^{-i\omega(t-nT_s)}\left(\int_{-\infty}^{\infty} q(y,z,\omega,k_x)e^{ik_x(x-x_0(nT_s))}dk_x\right)d\omega, \tag{7}$$

Here, it is important to note that the number of 2.5D integrals is rather high depending on the duration of the signal and the source signal sampling frequency. Since the 2D-BEM calculations itself as well as the inverse Fourier transform for k_x are approximations, the question arises, whether a certain degree of interpolation suffices for this purpose.

As e.g. for the use in a perception experiment the signal of interest needs also to be sampled, the inverse Fourier transform can also be formulated in terms of a inverse DFT (with a potentially different sampling time T_r):

$$p(\mathbf{x},m) = \frac{1}{2\pi}\frac{T_s}{MT_r}\sum_{l=0}^{L-1}\sum_{n=0}^{N-1} s(nT_s)e^{-i\omega_l((T_0+mT_r)-nT_s)}\left(\frac{1}{2\pi}\int_{-\infty}^{\infty} q(y,z,\omega_l,k_x)e^{ik_x(x-x_0(nT_s))}dk_x\right), \tag{8}$$

Essentially, this is a formulation to evaluate the two integrals using a rectangular rule where T_s and $(MT_r)^{-1}$ are the step sizes of the forward and inverse Fourier transform, respectively. If $T_s = T_r$ this factor is simply the typical normalizing constant M^{-1} for an inverse DFT.

2.3.1 Interpolation

Each term in the double sum requires the standard 2.5D calculation. Considering signals of durations of a few seconds as well as typical sampling frequencies in audio applications a very large number of 2.5D calculations is necessary. For example, for a real signal of 1 s at 48 kHz, 24000 times 48000 inverse Fourier transforms (integral in parenthesis in Eq. 8) need to be evaluated. There is, however, a fundamental difference between the temporal and the spectral sum. For the time index n each value simply requires the calculation of different longitudinal offsets, i.e. positions along the x-axis using the set of 2D-BEM calculations for the given frequency ω_l. In contrast, each frequency value requires the calculation of a new set of 2D-BEM problems, which in general takes much longer. Thus, in particular interpolation over 3D-frequencies ω_l is important. As in the 2.5D case, a demodulation approach which allows to reduce the number of necessary quadrature points also works for this setting. An extreme example is the moving point source in free space $e^{ik_l r_n}(4\pi r_n)^{-1}$ where r_n is the distance between source and receiver at time n. When demodulating this with $e^{-ik_l r_n}$ the r_n-dependence is relatively smooth as long as the minimal source-receiver distance becomes not too small and the frequency dependence is a constant. Interpolating the real and imaginary part over r_n and/or k to a high accuracy hence becomes quite simple. Having a reflecting half space the problem becomes more interesting, as the 3D-solution is given as

$$\frac{1}{2\pi}\int_{-\infty}^{\infty} q(y,z,\omega_l,k_x)e^{ik_x x_n}dk_x = \frac{e^{ik_l\sqrt{x_n^2+(y-y_0)^2+(z-z_0)^2}}}{4\pi\sqrt{x_n^2+(y-y_0)^2+(z-z_0)^2}} + \frac{e^{ik_l\sqrt{x_n^2+(y-y_0)^2+(z+z_0)^2}}}{4\pi\sqrt{x_n^2+(y-y_0)^2+(z+z_0)^2}} \tag{9}$$

From this, it is clear that there is no optimal demodulation due to two superimposed and different oscillations.

2.4 Evaluation

Although the methods described earlier allow for a non-uniform motion as well as wide-band signals, uniform motion and a mono-frequent stimulus was used for an initial evaluation. As an example to illustrate the potential savings on computation time, a moving point source above a reflecting half space will be used with 4 m source separation and source and receiver located 0.5 m above the half plane. The smallest distance between source and receiver is at $t = 0$.

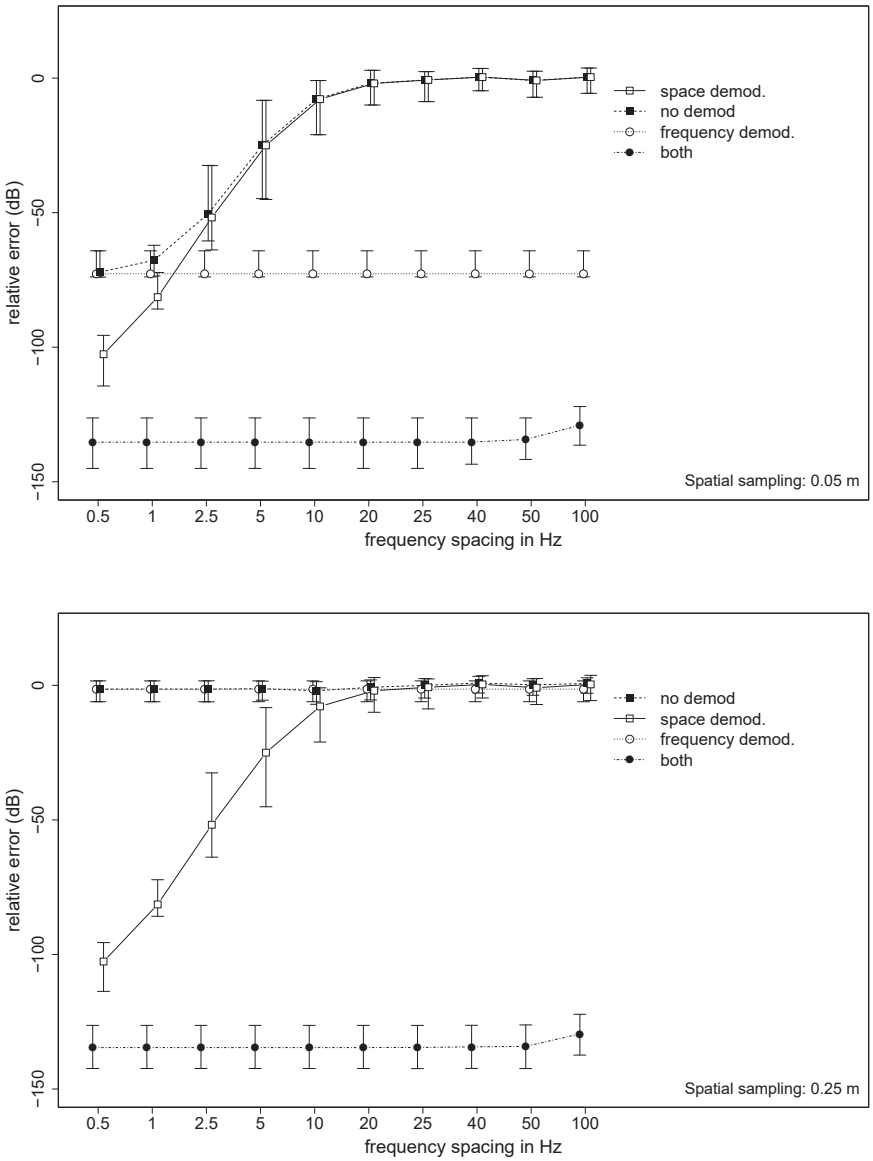

Figure 1. Effect of the demodulation. The figure illustrates the median and the inter-quartile-range (IQR) of the relative error in dB over time when compared to the reference solution. Different frequency spacings and demodulation settings for the interpolation are shown. The upper panel shows the results for a spatial sampling distance of 0.05 m, the lower panel shows the results for 0.25 m. The horizontal jitter for the same frequency spacing is only for visual clarity.

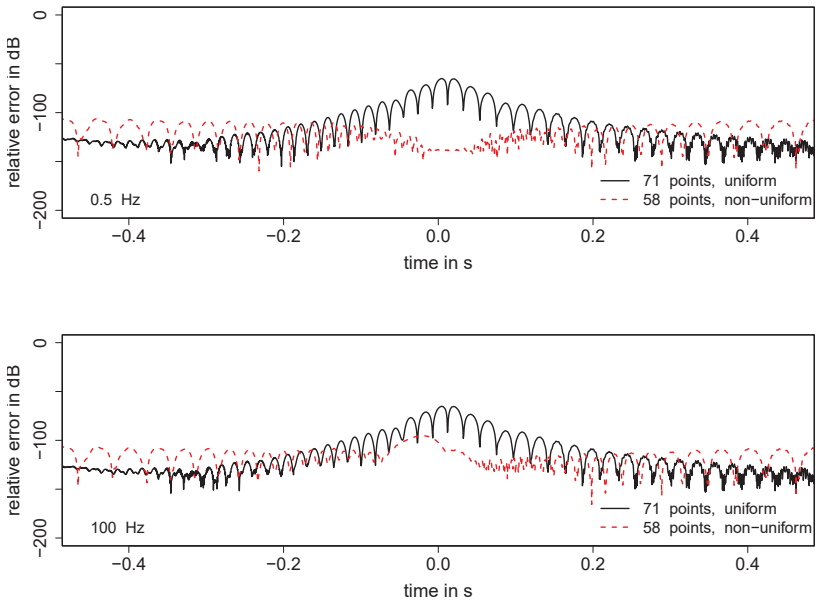

Figure 2. Temporal/spatial distribution of the error for coarse spatial sampling. The figure illustrates the relative error in dB as a function of time for a spatial sampling of 1 m and 0.5 Hz (upper panel) as well as 100 Hz (lower panel) spectral sampling distance. The line color denotes uniform (black) and non-uniform (red) sampling.

Different frequency as well as spatial spacings are compared in terms of deviations from the reference solution. A cubic spline was used for interpolation as implemented in the function *spline* of the R programming language [6]. The reference solution was calculated using the retarded potential formula (see e.g. [3]). The difference between the reference and the approach presented here is expressed in terms of the relative error expressed in dB. A data window was applied to the source signal to avoid potential problems at the endpoints of the signal. To exclude the data window from the analysis, 0.5 s at the beginning and the end of the receiver signal were discarded before the error was calculated.

3 RESULTS

The effect of the spatial as well as the spectral demodulation for different spectral sampling intervals is illustrated in the upper panel of Fig. 1 for a source speed of 50 m/s, a frequency of 800 Hz, a sampling frequency of 2000 Hz, and a spatial sampling distance of 0.05 m. Note, that a full sampling would necessitate the calculation of 2.5D transfer functions every 0.025 m.

The effect of spectral demodulation is apparent. Due to the full signal length of 2.5 s in the calculation the theoretical spacing is 0.4 Hz. When increasing the spectral spacing the error increases steadily unless demodulation is applied. Since the spatial sampling is coarser than required in theory, using spatial demodulation also results in a reduction of the relative error. When increasing the sampling distance (0.25 m, lower panel Fig. 1), spatial demodulation becomes more important.

Eventually, for yet a coarser sampling the error starts to increase even in the demodulated setting. Fig. 2 illustrates the relative error over time for a spatial sampling at 1.0 m and two different spectral sampling intervals (0.5 Hz upper panel, 100 Hz lower panel, solid black lines).

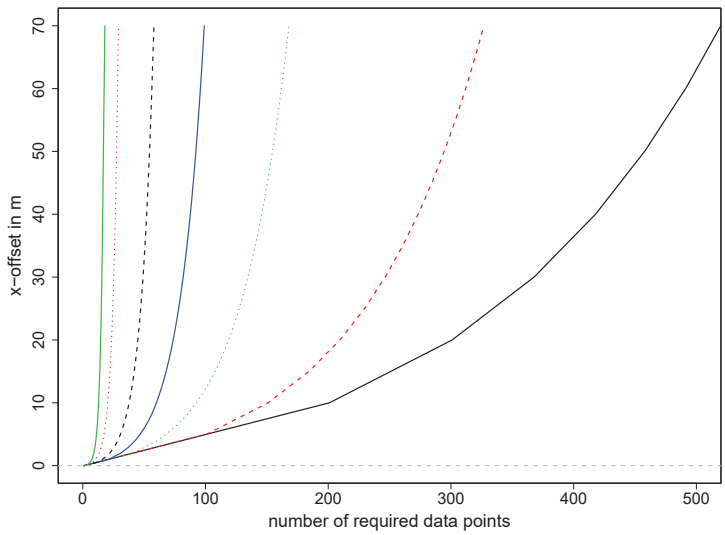

Figure 3. Non-uniform sampling. The figure illustrates the number of points required to sample up to a given x-offset for the different non-uniform sampling functions as distinguished by line type and color.

From this figure it can be seen that the frequency sampling has a only a minor effect due to the use of the spectral demodulation. The uniform spatial sampling leads to an increased error when the source is in the vicinity of the receiver, as the change of change in the spectrum as a function of position is higher. Thus, in this region a denser sampling is required. A non-uniform spatial sampling has been used, where the spacing of the data points used for interpolation is proportional to the distance in x between the source and the receiver. Fig. 3 illustrates this sampling for different proportionality factors. It can be seen that the region with smaller offsets is more densely sampled. Fig. 2 (dashed red lines) shows, that the error can be controlled by using a non-uniform sampling density, although the sampling towards higher offsets was chosen too coarse in this case.

4 CONCLUSIONS

This preliminary work deals with the potential saving on computation time when dealing with moving sources in acoustic scattering. Results on a uniformly and mono-frequent moving point source above a reflecting half-space show that the number of data points for which the BEM needs to be calculated can be reduced significantly when using a demodulation approach before interpolation. For a single frequency and constant motion, the presented approach may not be optimal. However, the method is applicable to more general situations and initial data on non-uniform motion also show increased efficiency when using spatial and spectral interpolation. The example illustrated did not involve a scatterer and thus only required the calculation of the Green's function instead of real 2D BEM calculations. Preliminary data on a noise barrier example indicate similar tendencies although higher overall errors were observed. However, a thorough analysis of different settings is necessary. Furthermore, other interpolation methods than a cubic spline may also be more efficient.

REFERENCES

[1] C. H. Kasess, W. Kreuzer, and H. Waubke. Deriving correction functions to model the efficiency of noise barriers with complex shapes using boundary element simulations. *Applied Acoustics*, 102:88 – 99, 2016.

[2] C. H. Kasess, H. Waubke, M. Conter, C. Kirisits, R. Wehr, and H. Ziegelwanger. The effect of railway platforms and platform canopies on sound propagation. *Applied Acoustics*, 151:137 – 152, 2019.

[3] D. Duhamel. Efficient calculation of the three-dimensional sound pressure field around a noise barrier. *Journal of sound and vibration*, 197(5):547–571, 1996.

[4] C. Kasess, W. Kreuzer, and H. Waubke. An efficient quadrature for 2.5D boundary element calculations. *Journal of Sound and Vibration*, 382:213–226, 2016.

[5] D. Duhamel and P. Sergent. Sound propagation over noise barriers with absorbing ground. *Journal of sound and vibration*, 218(5):799–823, 1998.

[6] R Core Team. *R: A Language and Environment for Statistical Computing*. R Foundation for Statistical Computing, Vienna, Austria, 2018.